JOURNAL OF Materials CHEMISTRY
Communication

A novel enhancement of ionic conductivity in the cation-deficient apatite $La_{9.33}(SiO_4)_6O_2$

E. J. Abram, D. C. Sinclair and A. R. West

Department of Engineering Materials, Sir Robert Hadfield Building, University of Sheffield, Mappin Street, Sheffield, UK S1 3JD

Received 4th May 2001, Accepted 6th June 2001
First published as an Advance Article on the web 25th June 2001

Al can be doped into the oxide ion conductor $La_{9.33}(SiO_4)_6O_2$ according to the formula $La_{9.33+x/3}(SiO_4)_{6-x}(AlO_4)_xO_2$ where $0 \leqslant x \leqslant 2$; a conductivity enhancement of 1–2 orders of magnitude is observed for intermediate x values and illustrates the important role that La vacancies have in optimising the conductivity.

A wide variety of materials crystallise in the apatite structure (mineral formula $A_{10}(MO_4)_6X_2$), for example, fluoro-, chloro- and hydroxy-apatites[1] ($Ca_{10}(PO_4)_6X_2$ where X = F, Cl or OH), oxyapatites[2] ($Ca_8La_2(VO_4)_6O_2$), 'anion-deficient' apatites[3] ($Pb_8K_{2-x}Na_x(PO_4)_6$) and 'cation-deficient' apatites[4] ($La_{9.33}(SiO_4)_6O_2$). The apatite structure consists of isolated MO_4 tetrahedra with the remaining anions, X, occupying tunnels along the *c*-axis that allow easy diffusion of anionic species, such as F^-, Cl^-, OH^- and O^{2-}. As a consequence, many apatites are well-known one-dimensional anionic conductors.[5,6] The structure also contains tunnels through which cations may form percolation pathways and diffuse along the *c*-axis which can result in mixed cation/anion conduction.[7]

Rare-earth (RE)-based apatites have recently attracted considerable attention because of their high oxide ion conductivity.[8,9] Various stoichiometries have been investigated, including the stoichiometric composition, $(RE_{0.8}AE_{0.2})_{10}(MO_4)_6O_2$, 'cation-deficient' compositions, $RE_{9.33}(MO_4)_6O_2$, and 'oxygen-excess' compositions, $RE_{10}(MO_4)_6O_3$ and $(RE_{10-x}AE_x)(MO_4)_6O_{3-x/2}$ where RE = La, Nd, Sm, Gd, Dy, AE = Ca, Sr, Ba and M = Si, Ge. Stoichiometric and cation-deficient compositions can be prepared as single-phase materials; however, it has proved difficult to prepare phase-pure oxygen-excess compounds, especially those based on $RE_{10}(MO_4)_6O_3$.[8,10] To date, the highest oxide ion conductivities reported are for La-based oxygen-excess compositions such as $La_{10}(GeO_4)_6O_3$, $La_9Sr(GeO_4)_6O_{2.5}$, $La_{10}(SiO_4)_6O_3$ and $(La_{9.75}Sr_{0.25})(SiO_4)_6O_{2.895}$ despite uncertainties over their composition and phase purity. They have conductivities comparable to or better than that of yttria-stabilised zirconia, YSZ, at 600 °C, exhibit high oxygen ion transference numbers (>0.9) over a wide oxygen partial pressure range,[9] $1–10^{-21}$ atm, and the low activation energy (0.6–0.8 eV) associated with the oxide ion conduction makes them potentially useful low/intermediate temperature solid electrolytes.

At present, the structure–composition–property relationships of RE-based apatites are poorly understood; in particular, the conduction mechanism is unknown which makes it difficult to develop doping strategies to optimise their conductivity. A recent neutron diffraction study on $La_{9.33}(SiO_4)_6O_2$ by Sansom *et al.*[11] has shown that a significant concentration of oxygen ions (~14%) are displaced from the ideal channel site into a new interstitial site, thus creating Frenkel-type defects. This ion displacement was not observed for $La_8Sr_2(SiO_4)_6O_2$, which has much lower conductivity than $La_{9.33}(SiO_4)_6O_2$, and led Sansom *et al.*[11] to suggest that A-site cation vacancies may cause local distortions which provide the driving force for the displacement of some channel oxygen ions into interstitial sites. High oxide ion conductivity in these materials may therefore occur by an interstitial mechanism, as opposed to an oxide ion vacancy mechanism in doped-fluorite and perovskite-based oxide ion conductors such as YSZ and doped-lanthanum gallates.

In this communication, we report a novel enhancement of conductivity in $La_{9.33}(SiO_4)_6O_2$ by Al-doping which results in conductivities comparable to those of the oxygen-excess composition $La_{10}(SiO_4)_6O_3$. Possible origins of the conductivity enhancement are discussed.

Partial phase diagram studies on the La_2O_3–SiO_2–Al_2O_3 system at 1700 °C showed that Si can be partially replaced by Al in $La_{9.33}(SiO_4)_6O_2$ with charge compensation *via* incorporation of La according to the mechanism

$$Si^{4+} \Rightarrow Al^{3+} + 1/3La^{3+}$$

and general formula $La_{9.33+x/3}(SiO_4)_{6-x}(AlO_4)_xO_2$ where $0 \leqslant x \leqslant 2$. The solid solution is more extensive than the range $0 \leqslant x \leqslant 1$ at 1300 °C reported by Mazza *et al.*,[12] suggesting the solid solution limit is temperature dependent. All samples were prepared by the mixed oxide route from dried reagents of La_2O_3 (Aldrich, 99.99%), SiO_2 (Alfa Aesar, 99.5%) and Al_2O_3 (Alpha Aesar, 99.9%). Appropriate quantities of the reagents to give a batch weight of 5–10 g were milled in an agate planetary ball mill in acetone, pelleted, calcined overnight at 1300 °C, ground in an agate mortar and pestle in acetone, ball-milled, pelleted, and heated overnight at 1450 °C. This procedure was then repeated at 1700 °C. Phase-purity was confirmed by a combination of X-ray Diffraction, Scanning Electron Microscopy and Electron Probe Micro-Analysis. Ceramics sintered at 1700 °C had ~95% of the theoretical X-ray density; they were electroded with sputtered Au and the conductivity measured using Impedance Spectroscopy (Hewlett Packard model HP4192A) over the frequency range 5 Hz to 13 MHz with an applied voltage of 100 mV.

All XRD patterns were fully indexed using the space group $P6_3/m$ and the variation in lattice parameters with La content is shown in Fig. 1. Both a and c increase with La content in accordance with Vegard's law and the small volume expansion of the unit cell is consistent with the increasing La content. Impedance complex plane, Z'' *vs.* Z', plots consisted of at least two overlapping arcs and a low frequency 'spike' with an associated capacitance of a few μF. The spike is attributed to ionic polarisation and diffusion-limited phenomena at the Au electrode associated with the ionic conduction in these

DOI: 10.1039/b104006p

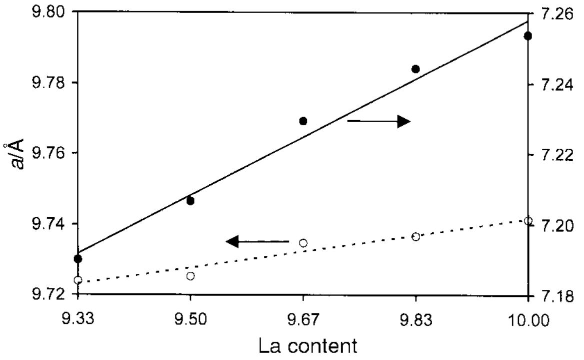

Fig. 1 Lattice parameters of Al-doped $La_{9.33}(SiO_4)_6O_2$ as a function of composition.

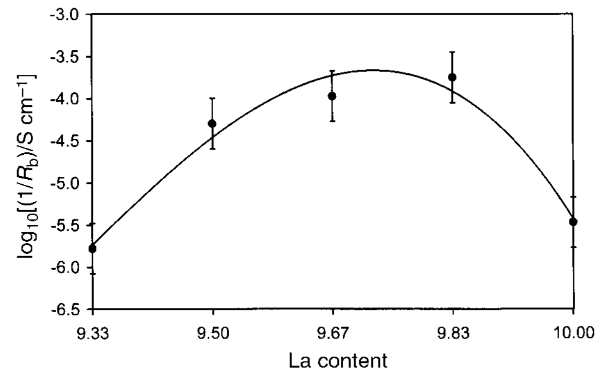

Fig. 3 Variation of bulk conductivity with La content at ~300 °C for Al-doped $La_{9.33}(SiO_4)_6O_2$.

materials. Detailed analysis of impedance spectroscopy data will be reported elsewhere; here we report bulk conductivities, σ_b, only where $\sigma_b = 1/R_b$ [R_b is the bulk resistance (corrected for sample geometry)]. R_b was extracted from the intercept of the high-frequency arc with the real, Z', axis. The associated capacitance of the high-frequency arc was calculated to be a few pF using the relationship $\omega RC = 1$ at Z''_{max}, (where ω is the angular frequency and $\omega = 2\pi f$, where f is the applied frequency) which is consistent with its assignment to the bulk response.

Bulk conductivity data for all samples are shown in Arrhenius format in Fig. 2 and reveal several features. First, the conductivity and activation energy (~0.8 eV) for $La_{9.33}(SiO_4)_6O_2$ are similar to those reported by other groups.[8–11] Second, there is a substantial increase in bulk conductivity by 1–2 orders of magnitude for compositions of intermediate x. Third, the highest conductivity, obtained for $La_{9.83}(SiO_4)_{4.5}(AlO_4)_{1.5}O_2$ ($x = 1.5$), is comparable to that reported for the oxygen-excess composition '$La_{10}(SiO_4)_6O_3$'. Fourth, all doped-samples show a change in slope at ~250 °C in their Arrhenius plot with activation energies of ~0.6 eV and 0.7 eV above and below this temperature respectively. Finally, the end members, $La_{9.33}(SiO_4)_6O_2$ and $La_{10}(SiO_4)_2(AlO_4)_2O_2$, have similar conductivity but different activation energies. The variation in bulk conductivity across the solid solution at 300 °C is shown in Fig. 3.

The Al-doping mechanism permits vacant La sites in $La_{9.33}(SiO_4)_6O_2$ to be filled at a constant oxygen content with the Al-rich end-member $La_{10}(SiO_4)_4(AlO_4)_2O_2$ having fully occupied La sites. Phase diagram studies showed no evidence for the alternative plausible Al-doping mechanism,

$$Si^{4+} + 1/2O^{2-} \Rightarrow Al^{3+}$$

since any solid solutions formed by this mechanism would occur in a different region of the phase diagram to that observed. The novelty of our results is the conductivity enhancement that occurs on Al-doping *at a fixed oxygen content*. This suggests that either intermediate La-deficient compositions are mixed cation/anion conductors with La^{3+} ions contributing significantly to the conductivity for La-vacancy contents, V_{La} (per unit cell) in the range $0 < V_{La} < 0.67$, or that the oxygen ion mobility is strongly influenced by the La-vacancy content and is optimised at an intermediate value, ~0.17 V_{La} per unit cell for Al-doping ($x = 1.5$). Detailed structural and electrical characterisation is now in progress to establish the origin of this conductivity enhancement; however, this result is consistent with the suggestion that La vacancies can cause channel oxygen ions to be displaced into interstitial sites, create Frenkel-type defects and produce high oxide ion conductivity.[11] Our preliminary results illustrate that La-site vacancies play a significant role in optimising the conductivity of cation-deficient RE-based apatites and that partial replacement of Si by Al with charge compensation by La is a novel doping mechanism to vary the La content between 9.33 and 10.

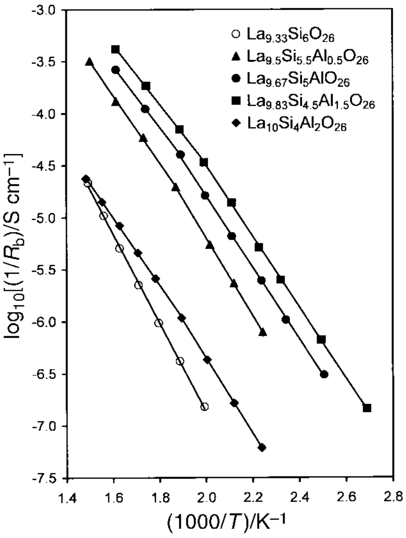

Fig. 2 Bulk conductivity data for Al-doped $La_{9.33}(SiO_4)_6O_2$.

Acknowledgements

We would like to thank the EPSRC for a studentship (E. J. A.).

Notes and references

1 J. C. Elliott, *Structure and Chemistry of Apatites and Other Calcium Orthophosphates*, Elsevier, Amsterdam, 1994.
2 H. Benmoussa, M. Mikou and J. L. Lacout, *Mater. Res. Bull.*, 1999, **34**, 1429.
3 L. H. Brixner and P. E. Bierstedt, *J. Solid State Chem.*, 1975, **13**, 24.
4 S. Nakayama, T. Kageyama, H. Aono and Y. Sadaoka, *J. Mater. Chem.*, 1995, **5**, 1801.
5 K. Yamashita, H. Owada, T. Umegaki, T. Kanazawa and T. Futagami, *Solid State Ionics*, 1988, **28–30**, 660.
6 T. Takahashi, S. Tanase and O. Yamamoto, *Electrochim. Acta*, 1978, **23**, 369.
7 A. Laghzizil, A. Bouhaouss, P. Barboux, R. Morineau and J. Livage, *Solid State Ionics*, 1993, **67**, 137.
8 S. Nakayama and M. Sakamoto, *J. Eur. Ceram. Soc.*, 1998, **18**, 1413.
9 H. Arikawa, H. Nishiguchi, T. Ishihara and Y. Takita, *Solid State Ionics*, 2000, **136–137**, 31–37.
10 S. W Tao and J. T. S Irvine, *Ionics*, 2000, **6**, 389.
11 J. E. H. Sansom, D. Richings and P. R. Slater, *Solid State Ionics*, 2001, **139**, 205.
12 D. Mazza and S. Ronchetti, *Mater. Res. Bull.*, 1999, **34**, 1375.